16[th] World Conference on Earthquake Engineering, 16WCEE 2017

Santiago Chile, January 9th to 13th 2017

Paper N° 3323

Registration Code: S-L1461143539

SEISMIC RELIABILITY OF BASE-ISOLATED STRUCTURAL SYSTEMS THROUGH FPS

P. Castaldo[(1)], B. Palazzo[(2)], G. Amendola[(3)]

[(1)] *Research Assistant, Dept. of Civil Engineering, University of Salerno, E-mail: pcastaldo@unisa.it*
[(2)] *Professor, Dept. of Civil Engineering, University of Salerno, E-mail: palazzo@unisa.it*
[(3)] *Graduate Student, Dept. of Civil Engineering, University of Salerno, E-mail: guglielmoamendola7@gmail.com*

Abstract

The paper deals with the seismic reliability of structural systems equipped with friction pendulum isolators (FPS). The behavior of these systems is analyzed by employing a two-degree-of-freedom model accounting for the superstructure flexibility, whereas the FPS isolator behaviour is described by adopting a widespread model which considers the variation of the friction coefficient with the velocity. The uncertainty in the seismic inputs is taken into account by employing a set of synthetic records, obtained through Monte Carlo simulations within the power spectral density method, with different characteristics depending on the soil dynamic parameters, and scaled to increasing intensity levels. The friction coefficient at large velocity is considered as random variable modeled through a uniform probability density function. Incremental dynamic analyses are developed in order to evaluate the probabilities exceeding different limit states related to both superstructure and isolation level defining the seismic fragility curves through an extensive parametric study carried out for different structural system properties. Finally, considering the seismic hazard curves related to L'Aquila site (Italy), the seismic reliability of the superstructure systems is evaluated as well as seismic reliability-based design (SRBD) abacuses are derived with the aim to design the radius in plan of the friction pendulum isolators in function of the structural system properties and the selected reliability level.

Keywords: FP devices; power spectral density method; medium soil condition; seismic fragility; seismic reliability.

1. Introduction

In the last decades, isolation systems have emerged as a very effective technique for the seismic protection of building frames [1], which, even if designed according to the most advanced codes, could suffer severe damages under strong earthquake events [2]. Among the base isolation devices currently employed for seismic isolation, friction pendulum system (FPS) isolators present some advantages, mainly related to their capability of providing an isolation period independent of the mass of the supported structure, their high dissipation and recentering capacity, and their longevity and durability characteristics [3]-[4].

Over the years, within the issue of the passive control, many works have developed new design strategies and methodologies [5]-[8], as well as other works have been focused on probabilistic analyses in structural dynamics, structural reliability methods, and reliability-based analysis. Reliability evaluation of base-isolated systems has been presented by Chen et al. [9], as well as Monte Carlo simulations have been performed by Fan and Ahmadi [10] to analyze the stochastic response of sliding isolation systems under random earthquake excitations. In Barroso and Winterstein [11], the seismic performance of steel buildings isolated with FPS bearings was evaluated by taking into account the variability of both the seismic intensity and the record characteristics. Seismic reliability analyses of a 3D system isolated by FPS bearings have been carried out in [12]-[14] by accounting for the randomness of both the isolator properties (i.e., coefficient of friction) and of the earthquake main characteristics. Performance curves for the isolators and the superstructure have been estimated by considering both the vertical and horizontal components of each seismic excitation. This way, a reliability criterion has been defined to assist the design of the isolator dimensions in plan by considering the effects of the uncertainties relevant to the problem according to seismic reliability-based design (SRBD) [15]. In [16]-[17], the influence of FPS bearing properties and of the structural parameters on the seismic performance of base-isolated structures through the nondimentionalitation of the motion of equations is analyzed by providing useful results for seismic reliability analyses, also defining optimal friction coefficient values for different soil conditions.

This paper deals with the seismic reliability of structural systems equipped with friction pendulum isolators (FPS) by presenting the fragility curves related to an extensive parametric study encompassing a wide range of building properties, seismic intensity levels and considering both the friction coefficient and soil characteristics as random variables. The isolated system is described by a two-degree-of-freedom (2dof) system in order to take account of the superstructure flexibility, and the FPS behavior is described by employing the model developed by Mokha et al. [4] for which the friction coefficient varies with the velocity. The uncertainty in the seismic inputs is taken into account by considering a set of artificial records [18], obtained through the power spectral density method [19], with different characteristics depending on soil dynamic parameters [20]-[21], and scaled to increasing intensity levels. Incremental dynamic analyses are developed in order to evaluate the probabilities exceeding different limit states related to both superstructure and isolation level through an extensive parametric study carried out for different structural properties. The estimates of the response statistics obtained are used for deriving seismic fragility curves of both the superstructure and isolation level assuming different values of the corresponding limit states. The seismic fragility curves are useful to evaluate the seismic reliability of base-isolated systems equipped with FPS, within the PEER-like modular approach [22]. In fact, in the final part of the work, considering the seismic hazard curve related to L'Aquila site (Italy), as provided by NTC08 [23], regarding a structural system isolated by FP bearings with a design life of 50 years, seismic reliability-based design (SRBD) abacuses are derived with the aim to design the radius in plan of the FP isolators in function of the structural properties and reliability level expected.

2. System Description and Equation of Motion

The equation of motion governing the response of a single-degree-of-freedom (SDOF) system on single concave FPS isolation devices to the seismic input $\ddot{u}_g(t)$ is:

$$\begin{aligned} m_s \cdot \ddot{u}_s(t) + c_s \cdot \dot{u}_s(t) + k_s \cdot u_s(t) &= -m_s \cdot \left[\ddot{u}_g(t) + \ddot{u}_b(t)\right] \\ m_b \cdot \ddot{u}_b(t) + f_b(t) + c_b \cdot \dot{u}_b(t) - c_s \cdot \dot{u}_s(t) - k_s \cdot u_s(t) &= -m_b \cdot \ddot{u}_g(t) \end{aligned} \tag{1}$$

where u_s denotes the displacement of the superstructure relative to isolation bearing, u_b the isolator displacement relative to the ground, m_s and m_b respectively the mass of the superstructure and of the basement, k_s and c_s respectively the superstructure stiffness and inherent viscous damping constant, c_b the bearing viscous damping constant, $\ddot{u}_g(t)$ the ground motion input, the dot differentiation over time, and where $f_b(t)$ denotes the FPS bearing resisting force. This latter can be expressed as:

$$f_b(t) = k_b \cdot u_b(t) + \mu(\dot{u}_b)(m + m_b)\, g Z(t) \tag{2}$$

where $k_b = (m_s + m_b) g / R$, g is the gravity constant, R is the radius of curvature of the FPS, $\mu(\dot{u}_b(t))$ the coefficient of sliding friction, which depends on the bearing slip velocity $\dot{u}_b(t)$, and $Z(t) = \mathrm{sgn}(\dot{u}_b)$, where sgn(·) is the sign function.

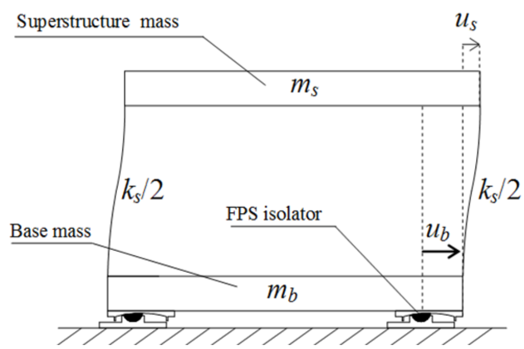

Fig. 1 – 2dof model of building isolated with FPS

Experimental results [4],[24]-[25] suggest that the coefficient of sliding friction of Teflon-steel interfaces obeys to the following equation:

$$\mu(\dot{u}_b) = f_{\max} - Df \cdot \exp(-\alpha |\dot{u}_b|) \tag{3}$$

in which $f_{\max}$ represents the maximum value of friction coefficient attained at large velocities of sliding, $f_{\min} = f_{\max} - Df$ represents the value at zero velocity.

In order to generalize the problem and unveil the characteristic parameters controlling the seismic behaviour of the system, the equation of motion can be reduced to a non-dimensional form. By dividing Eqn.(1a) by m_s, and Eqn.(1b) by m_b, Eqn.(1) can be rewritten as:

$$\begin{aligned} &\ddot{u}_s(t) + 2\xi_s\omega_s\dot{u}_s(t) + \omega_s^2 u_s(t) = -\left[\ddot{u}_g(t) + \ddot{u}_b(t)\right] \\ &\ddot{u}_b(t) + \frac{(m_s + m_b)}{m_b}\left[2\xi_b\omega_b \cdot \dot{u}_b(t) + \omega_b^2 \cdot u_b(t) + \mu(\dot{u}_b)\, g\, \mathrm{sgn}(\dot{u}_b)\right] - 2\xi_s\omega_s \cdot \frac{m_s}{m_b} \cdot \dot{u}(t) - \omega_s^2 \cdot \frac{m_s}{m_b} \cdot u(t) = -\ddot{u}_g(t) \end{aligned} \tag{4}$$

where the parameters ω_s and ξ_s denote the superstructure circular frequency and damping factor, whereas the parameters $\omega_b = \sqrt{\dfrac{k_b}{(m_s + m_b)}} = \sqrt{\dfrac{g}{R}}$ and ξ_b denote the fundamental circular frequency and damping factor for a rigid mass $(m_s + m_b)$ on a linear frictionless isolator of stiffness k_b and viscous damping constant c_b. The fundamental period of vibration of the base-isolated system, $T_b = 2\pi / \omega_b$, corresponding to the pendulum component, results to be independent of the superstructure mass and related only to the radius of curvature of the spherical surface *R*. After introducing the mass ratio $\gamma = \dfrac{m_s}{(m_s + m_b)}$ [26], Eqn.(4) can be rewritten as:

$$
\begin{aligned}
&\ddot{u}_s(t) + 2\xi_s\omega_s\dot{u}_s(t) + \omega_s^2 u_s(t) = -\left[a_g(t) + \ddot{u}_b(t)\right] \\
&\ddot{u}_b(t) + \frac{1}{1-\gamma}\left[2\xi_b\omega_b \cdot \dot{u}_b(t) + \omega_b^2 \cdot u_b(t) + \mu(\dot{u}_b)\, g\,\mathrm{sgn}(\dot{u}_b)\right] - 2\xi_s\omega_s\frac{\gamma}{1-\gamma}\cdot\dot{u}(t) - \omega_s^2\frac{\gamma}{1-\gamma}\cdot u(t) = -\ddot{u}_g(t)
\end{aligned}
\tag{5}
$$

3. Seismic Reliability of Structures with FPS : Random Variables

Seismic reliability assessment of a building structure, according to the structural performance (SP) evaluation method [12],[27], is based on the coupling between structural performance levels [28] and associated exceeding probabilities during its design life [29]. Coherently with the PEER-like modular approach [22] and performance-based earthquake engineering (PBEE) approach [30], the uncertainties related to the seismic input intensity are separated from those related to the characteristics of the record (record-to-record variability) by introducing a scale factor, i.e., an intensity measure (*IM*). The approach is based on calculating the probabilities of exceeding different limit state thresholds, properly defined, given different values of the intensity measure with the aim to define the fragility curves of the systems. Afterward, the abovementioned fragility curves integrated with the seismic hazard curve, expressed in terms of the same *IM*, related to a reference site, lead to the mean annual rates of exceeding the limit states. Using a Poisson distribution, it is possible to transform the mean annual rates of exceeding the limit states into probabilities of exceedance in the time frame of interest (e.g., 50 years).

The aim of this work consists of evaluating the seismic reliability of structural systems equipped with friction pendulum isolators (FPS) through an extensive parametric study encompassing a wide range of building properties, different seismic intensity levels and considering both the friction coefficient and earthquake characteristics as random variables.

With reference to the uncertainty in the seismic inputs, it is taken into account by considering a set of artificial records, obtained through the power spectral density (PSD) method [19] in order to evaluate the record-to-record variability of the structural system response. In particular, if the evolution of the frequency with the time can be neglected, each earthquake excitation can be modeled as a Gaussian stationary process with mean value equal to zero and two-sided power spectral density (PSD) function $S_{ff}(\omega)$. It follows that the stochastic process $f(t)$ can be simulated by the following series as $N \to \infty$:

$$f(t) = \sqrt{2}\sum_{n=0}^{N-1} A_n \cos(\omega_n t + \Phi_n) \tag{6}$$

where $A_n = (2S_{ff}(\omega_n)\Delta\omega)^{1/2}$, $\omega_n = n\Delta\omega$ for $n = 0 \ldots N-1$, $\Delta\omega = \omega_u / N$, having assumed $T_0 = 2\pi/\Delta\omega$=31.25s (NTC08) and $\omega_u = 50 rad/s$, $\Phi_0, \Phi_1, \Phi_2, \ldots\ldots, \Phi_{N-1}$ are independent random phase angles distributed uniformly over the interval [0,2π]. A sample function $f^{(i)}(t)$ of the simulated stochastic process $f(t)$ can be obtained by replacing the sequence of random phase angles $\Phi_0, \Phi_1, \Phi_2, \ldots\ldots, \Phi_{N-1}$ with their respective *i*-th realizations $\Phi_0^i, \Phi_1^i, \Phi_2^i, \ldots\ldots, \Phi_{N-1}^i$, sampled through Monte Carlo simulations:

$$f^i(t) = \sqrt{2}\sum_{n=0}^{N-1} A_n \cos(\omega_n t + \Phi_n^i) \tag{7}$$

In this study, 100 sequence of random phase angles are sampled through Monte Carlo simulations in order to generate 100 input accelorometric signals. The power spectral density function (PSD) of the embedded stationary process is described by the widely-used Kanai and Tajimi [31]-[32], modified according to Clough and Penzien [33], which applies:

$$S_f(\omega) = \frac{\omega_g^4 + 4\xi_g^2\omega_g^2\omega^2}{(\omega_g^2-\omega^2)+4\xi_g^2\omega_g^2\omega^2} \cdot \frac{\omega^4}{(\omega_f^2-\omega^2)+4\xi_f^2\omega_f^2\omega^2} S_0 \tag{8}$$

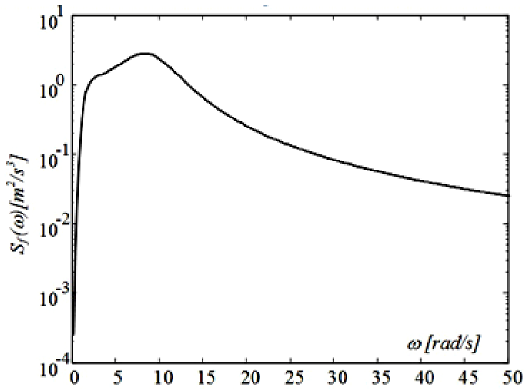

Fig. 2 – PSD function corresponding to Medium Soil condition

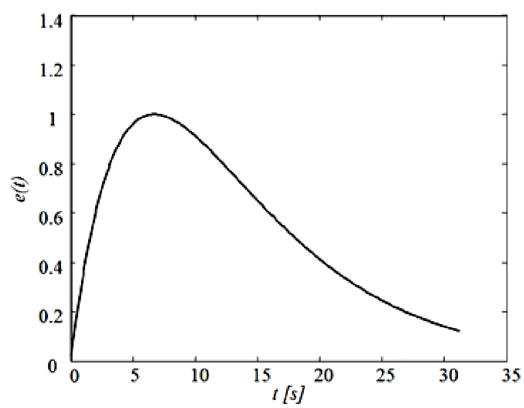

Fig. 3 – Time Modulating Function [35]

In the following parametric study, with the aim to assume the uncertainty related to earthquake characteristics in terms of soil dynamics parameters corresponding to Medium Soil condition according to EC8 [34], ω_g and ξ_g are modeled as random variables uniformly distributed, respectively, in the intervals [3π,5π] (rad/sec) and [40%,60%] [20]-[21], and sampled through Monte Carlo simulations. In Figure 2, the PSD function related to medium Soil with the sampled values of ω_g and ξ_g equal respectively to 3π and 40% is represented. In order to obtain non-stationary stochastic processes, a time-modulating function proposed by [35], as shown in Figure 3, is adopted.

Regarding the uncertainty of the friction coefficient at large velocity of the FP devices, the experimental data, developed by [4],[24]-[25] on sheet type Teflon bearings, have pointed out that friction is a complex phenomenon, not complying with the Coulomb friction law and that several mechanisms contribute to its variability. In this study, a uniform density probability function (PDF), ranging from 3% to 12%, has been assumed to model the sliding friction at large velocity as random variable f_{max}. For the generation of the sampled values of the friction coefficient f_{max}, within the stratified sampling techniques to develop Monte Carlo simulations, the Latin Hypercube Sampling (LHS) method [36]-[37] has been used. In particular, in the following parametric study, 20 sampled values *(j = 20)* of the random variable $f_{\max}$ are employed and assuming a ratio f_{max}/f_{min} equal to 3, based on regression of experimental results, whereas the exponent α of Eqn.(3) equal to 30 [4],[24]-[25].

4. Parametric Study: Incremental Dynamic Analysis Results

Seismic reliability assessment of the equivalent base-isolated systems is based on developing incremental dynamic analyses (IDA) [38].

4.1 Intensity Measure (IM): spectral displacement

In general, the *IM*'s choice should be driven by criteria of efficiency, sufficiency, and hazard computability [39]. In this study, the spectral displacement, $S_D(T_b, \xi_b)$, at the isolated period of the system, $T_b = 2\pi / \omega_b$, and for the damping ratio ξ_b, is assumed as intensity measure. In the analyses carried out in this study, the damping ratio ξ_b is taken equal to zero, consistently with [40]. The corresponding *IM*, hereinafter denoted as $S_D\left(T_b\right)$, in the IDA is assumed ranging from 0m to 0.5m.

4.2 Structural Parameters and Incremental Dynamic Analysis (IDA) results

The incremental dynamic analysis (IDA) is developed through an extensive parametric study encompassing a wide range of base-isolated building properties according to Eqn.(5). The parameters ξ_b and ξ_s are assumed respectively equal to 0% and 2%, γ equal to 0.7, the radius *R* of the FPS equal to 1m and 4m, the fixed-base system period T_s is considered varying between 0.3s and 1.5s. It follows that the isolation degree [41], ranges from 1.3 (flexible superstructure) to 13.3 (rigid superstructure).

The response parameters u_s and u_b are adopted as the engineering demand parameters (EDP). It follows that a set of samples is obtained for each output variable (EDP) representing the response variability. In this paper, the response parameters are assumed to follow a lognormal distribution according to [12]-[40]. A lognormal distribution can be fitted to the both response parameters (i.e., the extreme values of the EDPs), by estimating the sample lognormal mean, $\mu_{\ln}\left(EDP\right)$, and the sample lognormal standard deviation $\sigma_{\ln}\left(EDP\right)$, through the maximum likelihood estimation method.

In the hypothesis of regular buildings, the Eqn. (9), according to [23], is assumed as relationship between the fixed-base building period and its height *H*, and is employed to estimate the height *H* as the integer multiple of the inter-storey height assumed equal to *h*=3m and, so, the corresponding total number of floors N_f.

$$T_s = 0.075 H^{\frac{3}{4}} \tag{9}$$

For each $T_s = 2\pi / \omega_s$, assuming the building floor mass equal to $m_{s,i}$ = 1000 kNs^2/m, for $i=1 \ldots N_f$, it is possible to determinate the floor stiffness and vector Φ_1 containing the floor displacements of the first mode of the fixed-base structure normalized to the top floor displacement. The base mass m_b is assigned in order to respect the mass ratio γ [26]:

$$\gamma = \frac{\Gamma_1{}^2 M_{s1}}{\sum_{i=1}^{N_f} m_{s,i} + m_b} \tag{10}$$

where Γ_1 and M_{s1} represent respectively the participation factor and modal mass of the fundamental mode of the fixed-base structure. It follows that the maximum absolute inter-story drift of the 1st floor can be evaluated as $u_{s,1,\max} = \Gamma_1 \phi_{11} u_{s,\max}$, and this response parameter, divided by the inter-storey height assumed equal to *h*=3m, corresponds to the overall maximum interstorey drift index (IDI) experienced over the different stories that controls the performance of the superstructure and can be assumed as EDP.

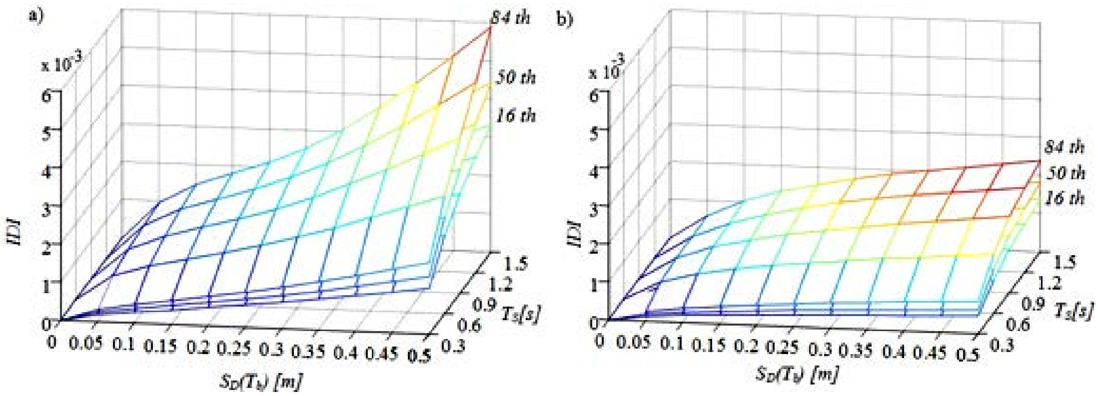

Fig. 4 – IDA curves of the superstructure 1st floor with γ=0.7, for R=1m (a) and R=4m(b)

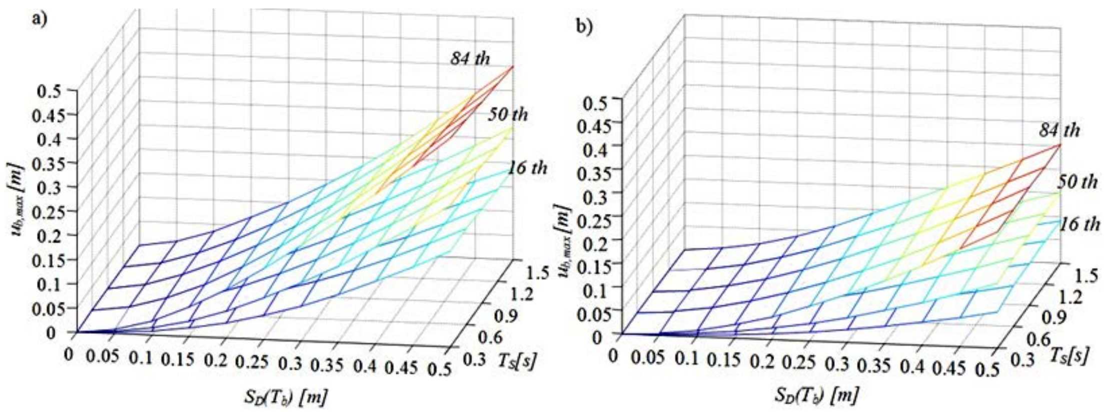

Fig. 5 – IDA curves of the isolation level with γ=0.7, for R=1m (a) and R=4m(b)

Fig.s 4-5 illustrate the IDA results regarding both the superstructure response in terms of IDI and the isolation level response u_b obtained for different values of the system parameters varying in the range of interest. Each figure contains several surface plots, corresponding to different values of percentile (50th, 84th and 16th). Fig. 4 shows the IDA results regarding the superstructure response. The lognormal mean and dispersion decrease for higher values of T_b and lower values of T_s (high value of the isolation degree). Fig. 5 shows the IDA results regarding the isolation level response u_b. The lognormal mean and dispersion also decrease for higher values of T_b (high value of the isolation degree) and for lower values of T_s.

5. Seismic Fragility of Structures with FP Devices

This section describes the evaluation of the probabilities p_f exceeding different limit states related to both the superstructure and the isolation level at each value of the *IM* defining the corresponding seismic fragility curves.

With reference to performance levels of the superstructure, four discrete performance levels or limit states (*LS1*,*LS2*,*LS3*,*LS4*), corresponding respectively to “fully operational”, “operational”, “life safety” and “collapse prevention” are provided from [28]. The performance limit states for base-isolated buildings, in accordance to provisions [42], have been defined by limiting the response of the lateral-load-resisting superstructure system, IDI limits, to a fraction of the limits provided for designing comparable fixed-base buildings [27].

In Table 1, the *LS1* and *LS2* thresholds assumed for the seismic fragility of the superstructure as well as the corresponding failure probabilities in a design life of 50 years are reported depending on the limit state. At each value of the intensity measure *IM*, the probabilities p_f exceeding different limit states related to the superstructure have been numerically computed for each considered combination of the superstructure/isolation level properties, as shown in Fig.s 6-7. With reference to the performance levels of the isolation system, several different values for the plan dimension of the isolator (i.e. radius in plan of the concave surface), are considered.

In Table 2, the limit state thresholds assumed for the seismic fragility of the FPS isolation level are reported.

Table 1 – Limit state thresholds for the superstructure [27]-[42]

	LS1 fully operational	*LS2 operational*
Inter-story drift (ISD) index	0.1%	0.2%
p_f *(50 years)*	$5.0 \cdot 10^{-1}$	$1.6 \cdot 10^{-1}$

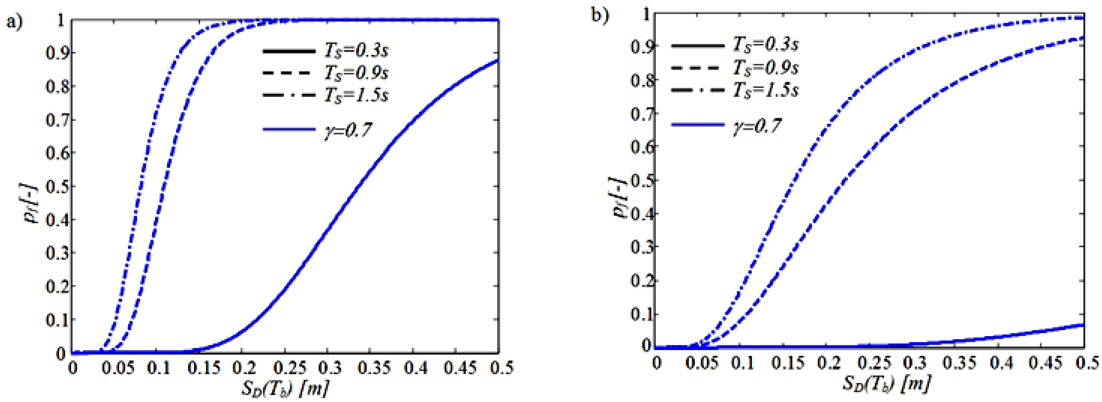

Fig. 6 – Seismic fragility curves of the superstructure 1st floor related to LS1, for R=1m (a), R=4m (b)

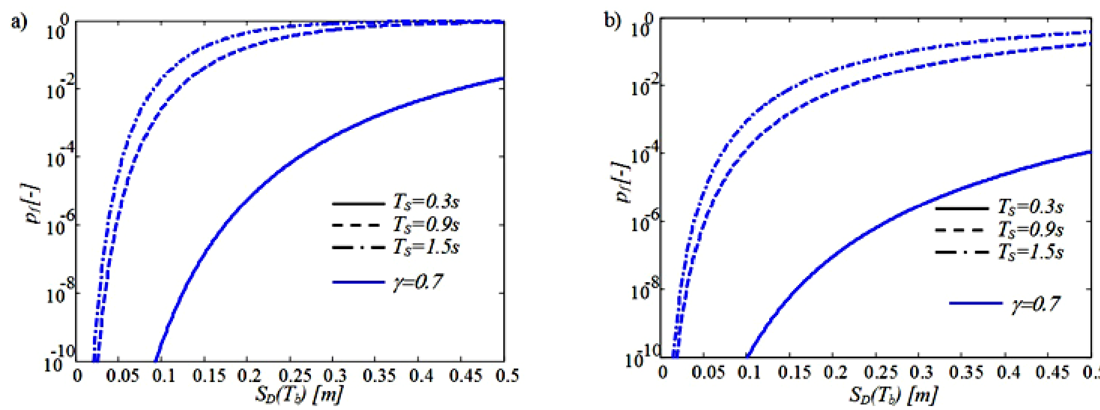

Fig. 7 – Seismic fragility curves of the superstructure 1st floor related to LS2, for R=1m (a), R=4m (b)

Table 2 – Limit state thresholds for the isolation level

	LS1	*LS2*	*LS3*	*LS4*	*LS5*	*LS6*	*LS7*	*LS8*	*LS9*
Maximum relative displacement [m]	0.1	0.15	0.2	0.25	0.3	0.35	0.4	0.45	0.5

Similarly, at each value of the *IM*, the probabilities p_f exceeding different limit states related to the isolation level have been numerically computed for each combination of the structural properties. Afterward, the abovementioned exceeding probabilities p_f have been fitted by a lognormal distribution. Fig.s 8-9 show the fragility curves regarding the isolation level for three values of T_s (0.3s, 0.9s and 1.5s) and two different values of the limit state thresholds: *LS5*-*LS9*. The seismic fragility of the isolation level increases for higher values of T_s.

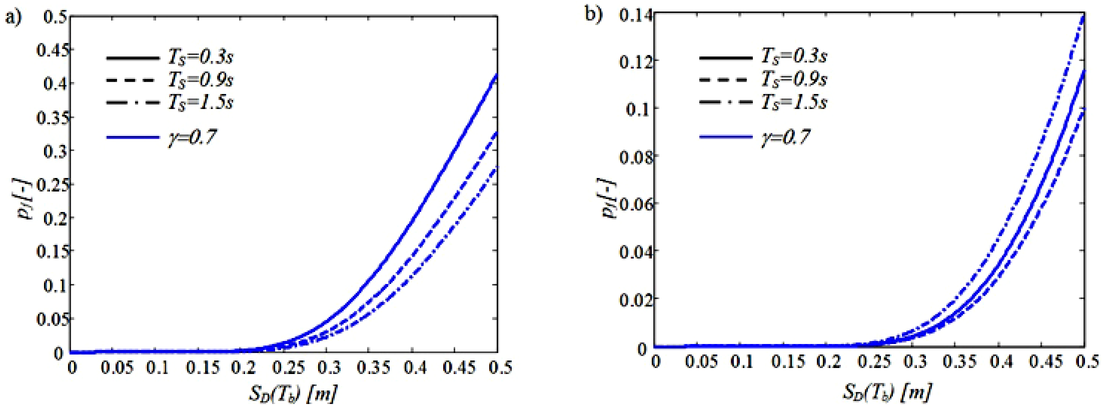

Fig. 8 – Seismic fragility curves of the isolation level related to *LS5*, for *R*=1m (a), *R*=4m (b)

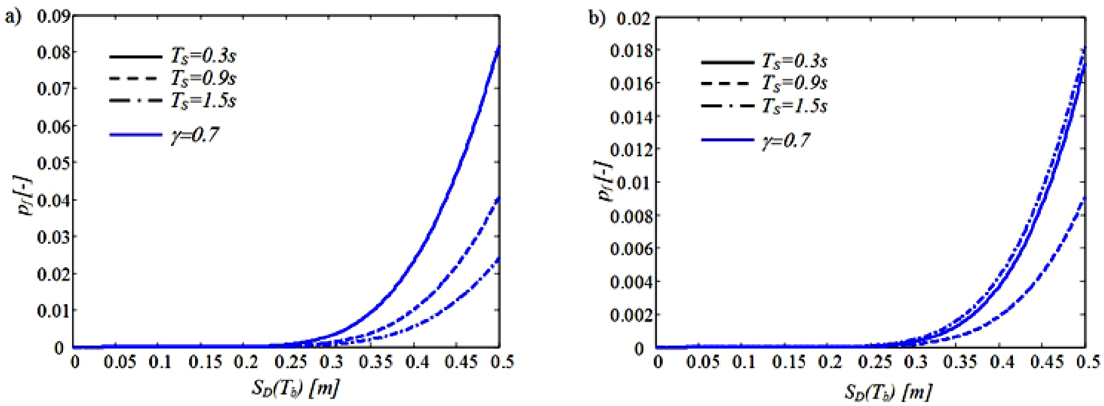

Fig. 9 – Seismic fragility curves of the isolation level related to *LS9*, for *R*=1m (a), *R*=4m (b)

6. Seismic Reliability of Structures with FP Devices

Considering L'Aquila site as the reference site, in Figure 10 the seismic hazard curves, expressed in terms of the same $IM = S_D(T_b)$, related to the different isolated periods analyzed in the parametric study are plotted according to NTC08. Each curve represents the average values of the annual rate λ of exceeding the $IM = S_D(T_b)$ level.

Integrating the fragility curves related to the superstructure with the seismic hazard curves and using a Poisson distribution, it is possible to evaluate the seismic reliability of the superstructure in the time frame of interest (50 years) for different values of the superstructure properties and having assumed the friction coefficient and soil dynamic parameters as random variables. The seismic reliability of the superstructure increases for low values of T_s (high values of the isolation degree), as shown in Figure 11. The results are consistent with those discussed by [12]. The seismic reliability of the isolation level decreases as *R* increases and slightly depends on the values of T_s (Fig. 12). Since the isolation level is not strongly influenced by the higher modes of the superstructure, the derived reliability-based abacuses are useful to design FP bearing devices depending on the properties of the superstructure and the expected reliability level in an area with a seismic hazard similar to that considered. In fact, an exceeding probability of $p_f = 1.5 \cdot 10^{-3}$ (related to collapse limit state, $\beta = 3$ in 50 years) is achieved through a radius in plan *r* ranging from about 0.2 m to about 0.4 m depending on system properties. The results are consistent with the monovariate structural performance curves in [12].

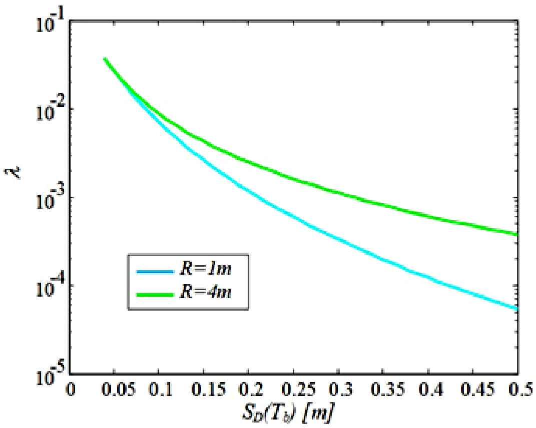

Fig. 10 – Seismic hazard curves related to the different isolated periods Tb for a site near L'Aquila (Italy)

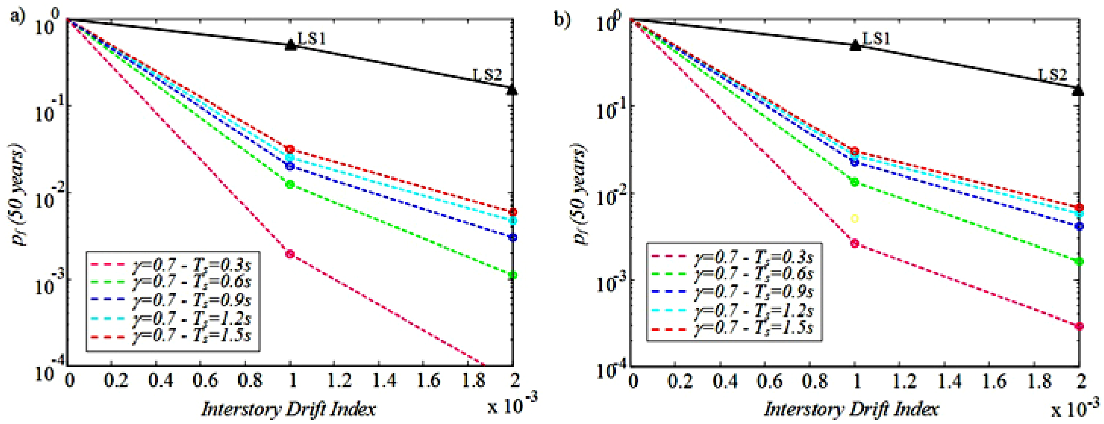

Fig. 11 – Seismic reliability curves of the superstructure 1st floor for R=1m (a), R=4m (b)

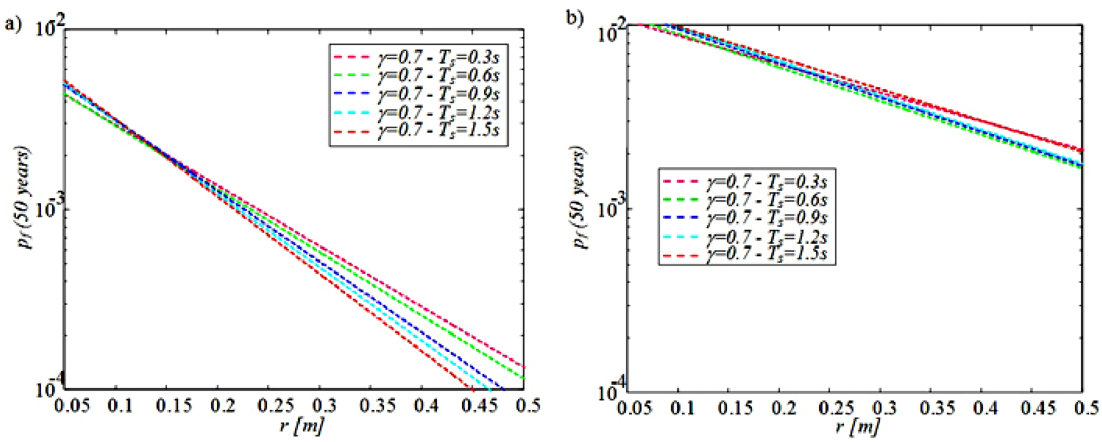

Fig. 12 – Seismic reliability curves of the isolation level for R=1m (a), R=4m (b)

7. Conclusions

This paper deals with the seismic reliability of structures equipped with FPS by presenting the fragility curves related to an extensive parametric study encompassing a wide range of building properties, different seismic intensity levels and considering both the friction coefficient and earthquake characteristics as random variables. The uncertainty in the seismic inputs is taken into account by considering a set of artificial records, obtained through the power spectral density method, with different characteristics depending on soil dynamic parameters. IDA are developed to evaluate the probabilities exceeding different limit states related to both superstructure and isolation level for different structural system properties. In the final part, considering the seismic hazard curve related to a site near to L'Aquila (Italy), according to NTC08, and regarding a structure isolated by FPS with a design life of 50 years, reliability-based abacuses are derived with the aim to design the radius in plan of the friction pendulum isolators.

8. References

[1] Christopoulos C, Filiatrault A (2006): *Principles of Passive Supplemental Damping and Seismic Isolation*. IUSS Press, Pavia, Italy.

[2] De Iuliis M, Castaldo P, Palazzo B (2010): Analisi della domanda sismica inelastica del terremoto de L'Aquila su sistemi dimensionati secondo le NTC2008. *Ingegneria Sismica,* Patron Editore XXVII (3), 55–68.

[3] Zayas VA, Low SS, Mahin SA (1990): A simple pendulum technique for achieving seismic isolation. *Earthquake Spectra*, 6, 317-333.

[4] Mokha A, Constantinou MC, Reinhorn AM (1990): Teflon Bearings in Base Isolation. I: Testing. *J. Struct. Eng*, **116** (2), 438-454.

[5] Castaldo P (2014): *Integrated Seismic Design of Structure and Control Systems*. Springer International Publishing, New York.

[6] Castaldo P, De Iuliis M (2014): Optimal integrated seismic design of structural and viscoelastic bracing-damper systems, *Earthquake Engineering and Structural Dynamics*, **43** (12), 1809–1827.

[7] De Iuliis M, Castaldo P (2012): An energy-based approach to the seismic control of one-way asymmetrical structural systems using semi-active devices. *Ingegneria Sismica - International Journal of Earthquake Engineering* XXIX (4), 31-42.

[8] Palazzo B, Castaldo P, Marino I (2015): The Dissipative Column: A New Hysteretic Damper. *Buildings*, **5**(1), 163-178.

[9] Chen J, Liu W, Peng Y, Li J (2007): Stochastic seismic response and reliability analysis of base-isolated structures. *J Earthquake Eng*, **11**, 903-924.

[10] Fan FG, Ahmadi G (1990): Random response analysis of frictional base isolation system. *J Eng Mech*, **116** (9), 1881 – 1901.

[11] Barroso LR, Winterstein S (2002): Probabilistic seismic demand analysis of controlled steel momentresisting frame structures. *Earthquake Engineering and Structural Dynamics*, **31** (12), 2049–2066.

[12] Castaldo P, Palazzo B, Della Vecchia P (2015): Seismic reliability of base-isolated structures with friction pendulum bearings. *Engineering Structures*, **95**, 80-93.

[13] Palazzo B, Castaldo P, Della Vecchia P (2015): Seismic reliability analysis of base-isolated structures with friction pendulum system. *IEEE Workshop on Environmental, Energy and Structural Monitoring Systems Proceedings*, Napoli.

[14] Castaldo P, Palazzo B, Della Vecchia P (2016): Life-cycle cost and seismic reliability analysis of 3D systems equipped with FPS for different isolation degrees, *Engineering Structures*, **125**;349–363.

[15] Castaldo P, Amendola G, Palazzo B (2016): Seismic fragility and reliability of structures isolated by friction pendulum devices: Seismic reliability-based design (SRBD), *Earthquake Engineering and Structural Dynamics*, DOI: 10.1002/eqe.2798.

[16] Castaldo P, Tubaldi E (2015): Influence of FPS bearing properties on the seismic performance of base-isolated structures. *Earthquake Engineering and Structural Dynamics* , **44** (15), 2817–2836.

[17] Castaldo P, Ripani M (2016): Optimal design of friction pendulum system properties for isolated structures considering different soil conditions, *Soil Dynamics and Earthquake Engineering*, **90**:74–87, DOI: 10.1016/j.soildyn.2016.08.025.

[18] Jangid R (2008): Stochastic Response of Bridges seismically isolated by friction pendulum system. *J. Bridge Eng*., **13** (4), 319-330.

[19] Shinozuka M, Deodatis G (1991): Simulation of stochastic processes by spectral representation. *Applied Mechanics Reviews*, **44** (4), 191-203.

[20] Pinto P, Giannini R, Franchin P (2004): *Seismic Reliability Analysis of Structures*. Iuss Press.

[21] Talaslidis DG, Manolis GD, Paraskevopoulos EA, Panagiotopoulos CG (2004): Risk analysis of industrial structures with hazardous materials under seismic input. *13^{th} World Conference on Earthquake Eng.*, Vancouver, B.C., Canada.

[22] Cornell CA, Krawinkler H (2000): Progress and challenges in seismic performance assessment. *PEER Center News*, **4**(1), 1-3.

[23] NTC08. Norme tecniche per le costruzioni. Gazzetta Ufficiale del 04.02.08, DM 14.01.08, Ministero delle Infrastrutture.

[24] Constantinou MC, Mokha A, Reinhorn AM (1990): Teflon Bearings in Base Isolation. II: Modeling. *J. Struct. Eng*.**,** **116** (2), 455-474.

[25] Constantinou MC, Whittaker AS, Kalpakidis Y, Fenz DM, Warn GP (2007): Performance of Seismic Isolation Hardware Under Service and Seismic Loading. *Technical Report MCEER-07-0012*.

[26] Kelly JM (1997): *Earthquake-Resistant Design with Rubber*. Springer-Verlag, *2^{nd} Edition*.

[27] Bertero RD, Bertero VV (2002): Performance-based seismic engineering: the need for a reliable conceptual comprehensive approach. *Earthquake Engineering and Structural Dynamics*, **31**, 627–652.

[28] SEAOC Vision 2000 Committee. Performance-based seismic engineering. Report prepared by Structural Engineers Association of California, Sacramento, CA., 1995.

[29] Saito T, Kanda J, Kani N (1998): Seismic reliability estimate of building structures designed according to the current Japanese design code. *Proceedings of the Structural Engineers World Congress*.

[30] Porter KA (2003): An overview of PEER's performance-based earthquake engineering methodology. *Proceedings of the 9th International Conference on Application of Statistics and Probability in Civil Engineering (ICASP9)*, San Francisco, California, 973-980.

[31] Kanai K (1957): Semiempirical formula for the seismic characteristics of the ground. *Bulletin of earthquake research institute* Vol. 35, 309-325.

[32] Tajimi H (1960): A statistical method of determining the maximum response of a building structure during an earthquake. *Proc., 2^{nd} World Conf. on Earthquake Eng*, Vol.II, 781-798.

[33] Clough RW, Penzien J (1993): *Dynamics of Structures*. McGraw-Hill, *2^{nd} Edition*.

[34] European Committee for Standardization. Eurocode 8-Design of Structures for Earthquake Resistance. Part 1: General Rules, Seismic Actions and Rules for Buildings, Brussels, 2004.

[35] Shinozuka M, Sato Y (1967): Simulation of nonstationary random process. *J. Engrg.Mech.Div*., **93** (1), 11-40.

[36] Mckey MD, Conover WJ, Beckman RJ (1979): A comparison of three methods for selecting values of input variables in the analysis from a computer code. *Technometrics* , **21**, 239-45.

[37] Celarec D, Dolsek M (2013): The impact of modelling uncertainties on the seismic performance assessment of reinforced concrete frame buildings. *Engineering Structures*, **52**, 340 – 354.

[38] Vamvatsikos D, Cornell CA (2002): Incremental dynamic analysis. *Earthquake Engineering and Structural Dynamics*, **31**(3), 491–514.

[39] Luco N, Cornell CA (2007), Structure-specific scalar intensity measures for near-source and ordinary earthquake ground motions. *Earthquake Spectra*, **23** (2), 357-92.

[40] Ryan KL, Chopra AK (2004): Estimation of Seismic Demands on Isolators Based on Nonlinear Analysis. *J. Struct. Eng.*, **130** (3), 392–402.

[41] Palazzo B (1991): Seismic Behavior of base-isolated Buildings. *Proc. International Meeting on earthquake Protection of Buildings*, Ancona.

[42] Building Seismic Safety Council (1997): NEHRP commentary on the guidelines for the seismic rehabilitation of buildings. Provisions (FEMA 274). Washington, DC.